



Opposite effects of successive hydration shells on the aqua ion structure of metal cations

Elizabeth C. Beret, Elsa Galbis, Rafael R. Pappalardo, Enrique Sanchez Marcos

► To cite this version:

Elizabeth C. Beret, Elsa Galbis, Rafael R. Pappalardo, Enrique Sanchez Marcos. Opposite effects of successive hydration shells on the aqua ion structure of metal cations. *Molecular Simulation*, 2009, 35 (12-13), pp.1007-1014. 10.1080/08927020903033125 . hal-00530456

HAL Id: hal-00530456

<https://hal.science/hal-00530456>

Submitted on 29 Oct 2010

HAL is a multi-disciplinary open access archive for the deposit and dissemination of scientific research documents, whether they are published or not. The documents may come from teaching and research institutions in France or abroad, or from public or private research centers.

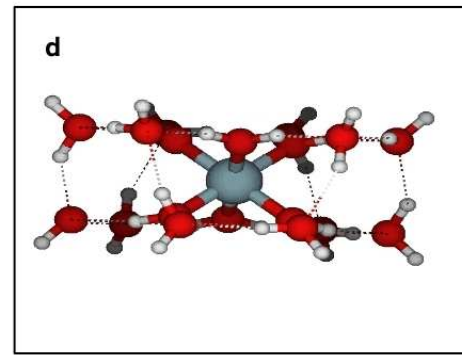
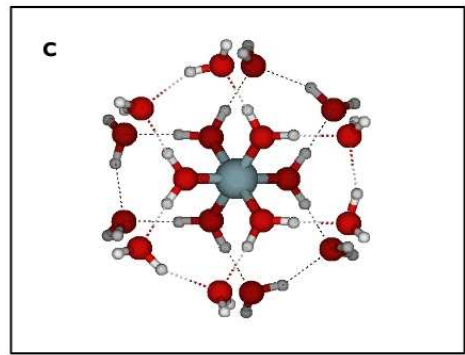
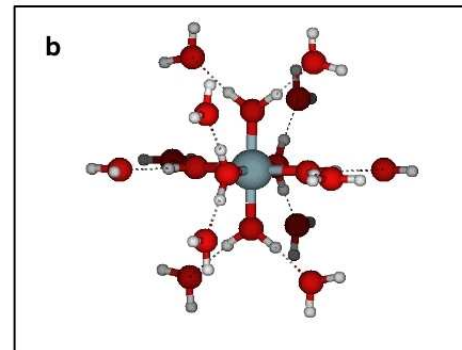
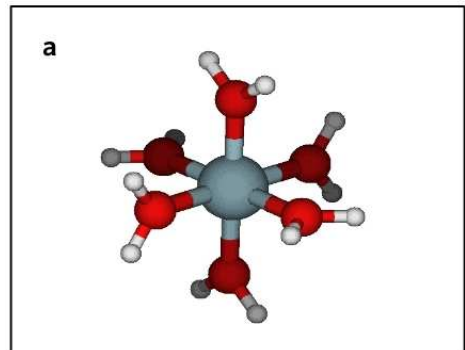
L'archive ouverte pluridisciplinaire **HAL**, est destinée au dépôt et à la diffusion de documents scientifiques de niveau recherche, publiés ou non, émanant des établissements d'enseignement et de recherche français ou étrangers, des laboratoires publics ou privés.



Opposite effects of successive hydration shells on the aqua ion structure of metal cations

Journal:	<i>Molecular Simulation/Journal of Experimental Nanoscience</i>
Manuscript ID:	GMOS-2009-0036.R1
Journal:	Molecular Simulation
Date Submitted by the Author:	23-Apr-2009
Complete List of Authors:	Beret, Elizabeth; Universidad de Sevilla, Quimica Fisica Galbis, Elsa; Universidad de Sevilla, Quimica Fisica Pappalardo, Rafael R.; Universidad de Sevilla, Quimica Fisica Sanchez Marcos, Enrique; Universidad de Sevilla, Quimica Fisica
Keywords:	Quantum Mechanics, CPMD, Mg(II), Al(III) aqua ions, Hydrogen bonding
Note: The following files were submitted by the author for peer review, but cannot be converted to PDF. You must view these files (e.g. movies) online.	
aquaion_supp.tex	

SCHOLARONE™
Manuscripts



238x181mm (100 x 100 DPI)

1
2
3
4
5
6
7
8
9
10
11
12 Opposite effects of successive hydration shells on the
13
14 aqua ion structure of metal cations
15
16
17
18
19

20 Elizabeth C. Beret, Elsa Galbis, Rafael R. Pappalardo
21
22 and Enrique Sánchez Marcos*

23
24 Departamento de Química Física, Universidad de Sevilla,
25
26 41012 Sevilla, Spain. e-mail:sanchez@us.es

27
28
29
30
31 Abstract
32

33 The conformation adopted by water molecules around a metal ion in aqueous
34 solution can be approached from a discrete representation of the solvent by studying
35 the structure and stability of microsolvation clusters including a different number
36 of water molecules. In this contribution we present a Quantum Mechanics and
37 ab initio Molecular Dynamics study on how the arrangement of water molecules
38 around Mg^{2+} and Al^{3+} shows preferentially a T_h or S_6 symmetry depending on
39 the number of hydration shells explicitly included in the calculation. The behavior
40 observed for both cases is the following: a) For a cluster composed of the metal ion
41 plus a first hydration shell the preferred geometry shows a T_h symmetry. b) When
42 a second hydration shell is added, a minimum can be found with a S_6 disposition of
43 water molecules around the metal center. c) However, if a third hydration shell is
44 considered a T_h arrangement of water molecules around the central ion is strongly
45 favored. The structures of the different solvation complexes studied in this work
46 are characterized. The preference for a T_h or S_6 distribution of water ligands is
47 rationalized in terms of total energies, interaction energies and the hydrogen bond
48 network.

1 Introduction

Aqua ions, of general formula $[M(H_2O)_n]^{m+}$, are the most common structures adopted by metal cations, M^{m+} , in water when chemical conditions inhibit the formation of hydrolyzed and polymerized derivatives.¹ The implicit net charge, $m+$, and the polar and polarizable character of water lead to electrostatic effects so strong that the perturbation exerted on the solvent goes beyond the formation of these coordination complexes or aqua ions, defining different solvation shells which surround the central metal cation. This picture of the hydration structure was firstly proposed by Frank and Evans and is regarded as the *concentric shells model*.² In a global sense the formation of the aqua ion is not enough to describe the behavior of an ion in solution, and the condensed medium effect has to be taken into account through different solvation shells and/or the bulk.

The structural information derived from experimental techniques for metal ions in aqueous solutions is restricted to one or two hydration shells solved by X-ray and neutron diffraction methods as well as X-ray absorption spectroscopies.^{1,3–6} NMR, Raman, IR and vis–UV techniques may also help in determining particular structural and dynamic properties.^{1,3,5} More recently, studies of small multivalent ion–water clusters in gas phase have been possible by a variety of techniques which supply both thermochemical and structural information.^{7–12} The characterization of increasingly large metal–water clusters is an important source of information not only for gas–phase ion chemistry, but it also allows the splitting of the solvent effects into specific and long-range contributions. Key structural parameters as coordination numbers vary from gas phase to solution, being a function of the cluster size.¹²

Theoretical methods may also provide a molecular description of the environment of a metal ion in water. From a quantum–mechanical point of view, there are three ways to represent the solvation of an ion in solution. In the discrete approach, a certain number of solvent molecules are explicitly included in the calculation in order to represent the intermolecular interactions between the ion and its closest solvent environment.¹³ In the

continuum approach, the solvent is represented in an averaged manner by a polarizable dielectric continuum, generally characterized by macroscopic properties of the pure liquid solvent.^{14,15} In the semi-continuum approach, the closest environment of the ion is represented by discrete water molecules, while the rest of the solvent is described by a continuum.^{16,17} The molecular description of the solvent has been tackled at two levels. On one hand, the use of force fields in order to perform computer simulations and molecular mechanics allows the inclusion of a significant number of solvent molecules, but representing the inter- and intramolecular interactions in a simplified form. On the other hand, a more refined description of the interactions can be achieved by the use of static quantum-mechanical calculations, although in this case the computational requirements are high and only a limited number of solvent molecules can be treated, typically up to two solvation shells. If more solvation shells are to be considered, the statistical factors become important in order to describe the solvent, and then it seems more appropriate to perform ab initio Molecular Dynamics (MD) simulations such as Born-Oppenheimer¹⁸ or Car-Parrinello MD.¹⁹

In the present study we aim to analyze the effect of successively increasing the number of hydration shells around two metal ions, Mg^{2+} and Al^{3+} , whose aqua ion structure in solution has been determined experimentally.^{1,3,20,21} It is well known that the first coordination shell of both Mg^{2+} and Al^{3+} is sixfold, the aqua ion exhibiting an average T_h symmetry in solution.

There are also theoretical studies on these metal ions within the discrete representation of the solvent. When the structure of the hexahydrate is quantum-mechanically optimized, i.e. only the metal ion and its first hydration shell are considered, in the absence of hydrolysis effects the resulting configurational minimum has a T_h symmetry^{22,23} (see Fig. 1a). Although at this level we are excluding a large amount of solvent effects, the structure of the aqua ion is already coherent with the known T_h structure that is found in solution.

Several configurational minima have been reported when two hydration shells are included in the calculation. First of all, a minimum with T_h symmetry can be found, in which the overall shape of the system is roughly spherical^{22,24} (Fig. 1b). Pye and Rudolph²⁵ find another minimum in which the second-shell water molecules are distributed into three interacting clusters (see Fig. 12 of Ref. 25). This structure has a lower energy than the T_h minimum. Bock *et al.*²⁶ find yet another minimum with S_6 symmetry, and lower in energy than the other two configurations (Fig. 1c,d). In this structure, the second-shell water molecules are arranged into the form of a crown surrounding the core hexahydrate, i.e. the overall shape of the system is no longer spherical. This result is striking since it does not fit the behavior expected for a metal hexahydrate in liquid water, as summarized by the concentric shells model of Frank and Evans. It is neither consistent with the description obtained from MD simulations of the ions in liquid water. In the present contribution we reexamine the evolution of the stability of the T_h and S_6 aqua ion conformers by successively increasing the number of hydration shells around the metal ion, combining static QM calculations and ab initio MD simulations. A careful analysis of their structures, relative energies and of their inter-shell interactions is needed to get insight into this problem.

2 Methods

Gas-phase quantum-mechanical (QM) optimizations have been performed for the structures of Mg^{2+} and Al^{3+} aqua ions including one and two hydration shells ($[M(H_2O)_6]^{m+}$ and $[M(H_2O)_{18}]^{m+}$, respectively). For each case the optimization started from two configurations, one with T_h and the other one with S_6 arrangement of ligands, and no symmetry restrictions were applied during the minimization process. In the one-shell complexes a single minimum was found, showing T_h symmetry. Inclusion of a second hydration shell allows the finding of two minima, having T_h and S_6 symmetry respectively.

When a third solvation shell is explicitly taken into account, the number of degrees

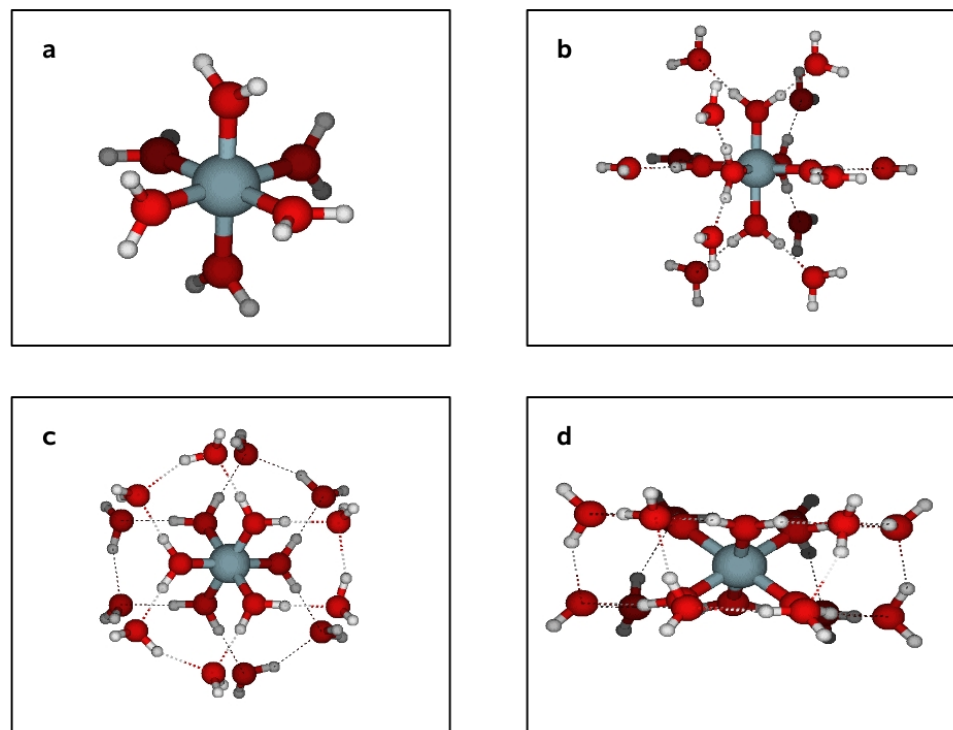


Figure 1: Representative configurations of the QM optimized structures of: a) $[M(H_2O)_6]^{m+}$ b) $[M(H_2O)_{18}]^{m+}$, T_h conformer c) and d) $[M(H_2O)_{18}]^{m+}$, S_6 conformer.

of freedom in the system increases to make a QM optimization of the structure hardly affordable in terms of computational costs. Furthermore, the shape of the potential energy surface (PES) includes a large number of local minima with similar energies, and it is difficult to reach a global minimum. Therefore we have employed an alternative strategy using ab initio Car-Parrinello Molecular Dynamics simulations¹⁹ (CP-MD) to obtain a configuration that, while being only a local minimum on the PES is representative of a T_h or S_6 arrangement of ligands in the second hydration shell of the aqua ion.

For each metal cation, Mg^{2+} and Al^{3+} , $[M(H_2O)_{42}]^{m+}$ initial configurations have been built by addition of 24 extra water molecules around the T_h and S_6 $[M(H_2O)_{18}]^{m+}$ minima using the Packmol code.^{27,28} The coordination number of 24 water molecules for the third shell was chosen in order to provide the minimum number of water molecules which may coordinate to the 12 second-shell water molecules by hydrogen bonding. An initial relaxation of the system has been performed by equilibration of the nuclei to a

1
2
3
4
5
6
7 low temperature (50 K) and during a short period of time (~ 0.4 ps) in order to avoid
8 strong deviations from the initial symmetry (T_h or S_6) within the $[M(H_2O)_{18}]^{m+}$ unit.
9 Afterwards an annealing procedure is applied, slowly diminishing the temperature of the
10 system by applying a reducing factor on the nuclei velocities at each MD simulation step,
11 until the temperature is below 5 K. Due to the thermal agitation experienced by the
12 system during this process, in the final conformation the inner $[M(H_2O)_{18}]^{m+}$ core does
13 neither maintain the initial symmetry nor is a minimum on the PES. However it is close
14 enough to be qualitatively representative of the T_h or S_6 coordination modes (see Fig. 2).

15
16
17 Gas-phase QM calculations and CP-MD simulations were performed using the CPMD
18 program package.²⁹ Norm-conserving Gaussian pseudopotentials of the Troullier–Martins
19 type³⁰ and a plane wave (*p.w.*) cutoff of 80 Ry were employed, applying cluster boundary
20 conditions³¹ to avoid spurious electrostatic coupling of periodic images of the charged
21 clusters. During the simulations the equations of motion were integrated using a time step
22 of 4 a.u. together with a fictitious electron mass parameter of 400 a.u. and the hydrogen
23 mass for H. All calculations were carried out with the PBE exchange and correlation GGA
24 functional.^{32,33}

3 Results and discussion

3.1 Comparison between plane waves and Gaussian functions

41
42 Previous QM calculations cited in the literature used Gaussian functions (*g.f.*) as basis
43 sets.^{22–26} In order to check the influence of *p.w.* or *g.f.* as a basis set, the gas-phase QM
44 optimizations of the structures containing one or two hydration shells were also performed
45 using the 6-311++G(2d2p) basis sets^{34,35} with the Gaussian03 code³⁶ using the same
46 PBE exchange and correlation GGA functional^{32,33} as for the *p.w.* calculations. The
47 interatomic distances using *p.w.* are larger than those obtained with *g.f.* (see Supporting
48 Information). The maximum differences are of circa 0.1 Å within the first hydration shell,

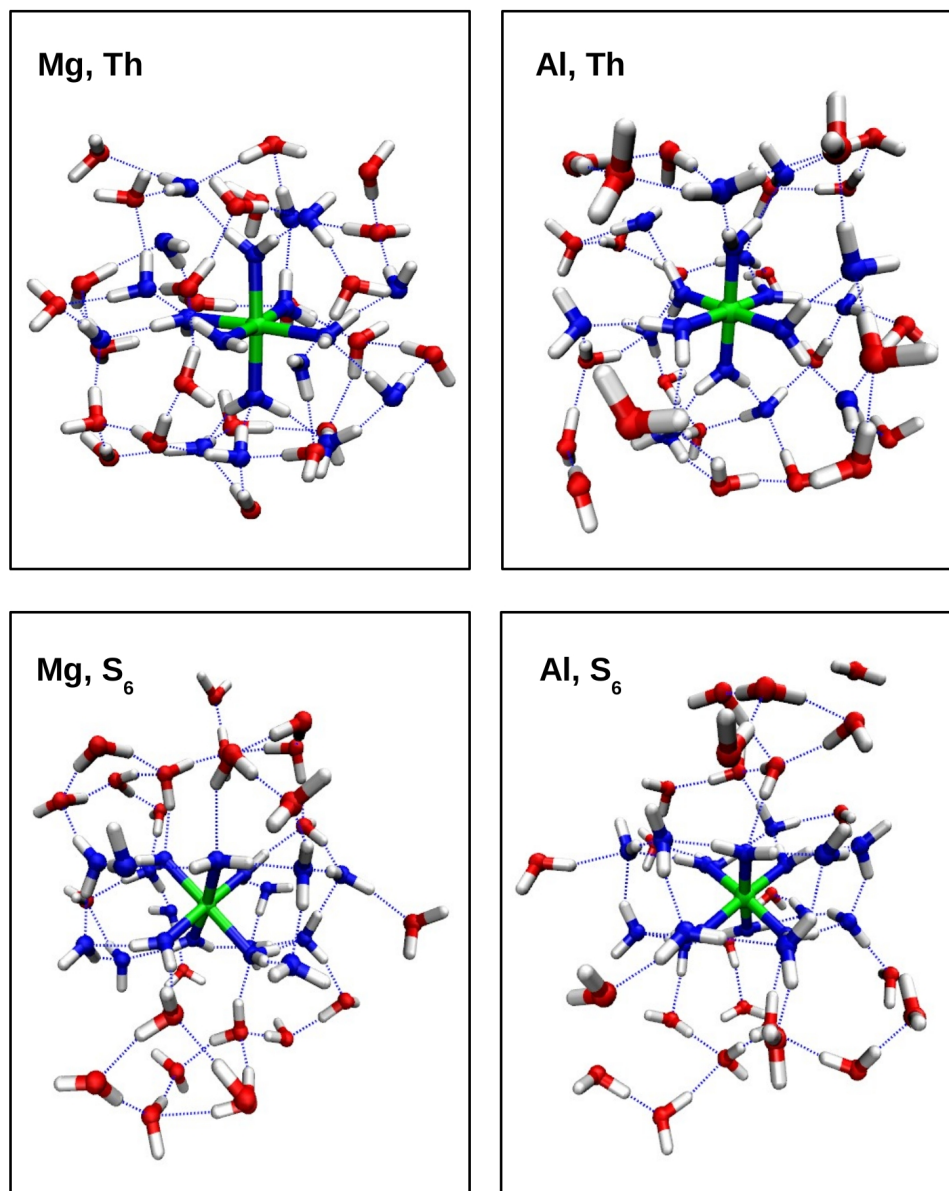


Figure 2: Final structures resulting from the annealing process for the $[\text{Mg}(\text{H}_2\text{O})_{42}]^{2+}$ and $[\text{Al}(\text{H}_2\text{O})_{42}]^{3+}$ clusters.

and somewhat larger in the second shell for the T_h structures. At least some hundredths of Å within this difference can be ascribed to the fact that *g.f.* are intrinsically affected of basis set superposition error while *p.w.* are not.³¹ However the inner description of H_2O in the first and second shells is not affected by the use of *p.w.* or *g.f.* Furthermore, the energy difference between the T_h and S_6 structures including the metal ion plus two solvation shells is the same, within 0.3 kcal/mol, if computed with *p.w.* or *g.f.* for both

Mg²⁺ and Al³⁺. Therefore *p.w.* provide a description equivalent to that obtained with *g.f.*, at least concerning the issues studied in this contribution, and only results obtained with the *p.w.* will be discussed in the rest of the paper.

3.2 Structural analysis

The [M(H₂O)₆]^{m+} and [M(H₂O)₁₈]^{m+} optimized structures for Mg²⁺ and Al³⁺ aqua ions (Fig. 1) and the final [M(H₂O)₄₂]^{m+} structures obtained from the annealing process (Fig. 2) are described in Table 1 by means of selected structural data. Overall, the resulting structures are in good agreement with the data available in the bibliography for these hydration complexes.^{1,3,22–26} In order to facilitate the visualization of the different *T_h* and *S₆* structures, the cartesian coordinates of the [M(H₂O)₁₈]^{m+} and [M(H₂O)₄₂]^{m+} clusters described in Table 1 have been included as Supporting Information.

The QM optimization of the [M(H₂O)₆]^{m+} structure yields a *T_h* arrangement of water molecules around the metal ion for both Mg²⁺ and Al³⁺. However, when a second hydration shell of water molecules is considered in the calculation, two minima can be found, with *T_h* and *S₆* symmetries, respectively. These two conformations are remarkably distinct from the geometrical point of view: in the *T_h* case, the water molecules in the first and second shells have a strong ion–dipole orientation towards the central cation (Fig. 1b) while for the *S₆* conformer the H atoms in the first shell are tilted from their ion–dipole orientation, allowing second–shell water molecules to arrange into the shape of a crown around the metal ion (Fig. 1c,d). Due to such an arrangement of water molecules, the distance from the metal to H atoms in the first shell is slightly shorter in the *S₆* conformer. This variation in the M–H_I distance translates into a more important difference concerning oxygen atoms in the second shell of the *S₆* arrangement: their distance to the central ion is circa 0.4 Å shorter in the case of Mg²⁺ and 0.2 Å for Al³⁺. Accordingly, the M–H_{II} distances are also shorter in the *S₆* than in the *T_h* conformers. The rest of structural parameters reported in Supporting Information are not influenced

Table 1: Selected interatomic distances (\AA) for the solvation complexes of Mg^{2+} and Al^{3+} including a different number of hydration shells. Average distances are given in the case of the $[\text{M}(\text{H}_2\text{O})_{42}]^{n+}$ clusters. Reference data from the literature (Refs. 1,3,22–26) are given in parenthesis.

System	Symmetry	$d_{(\text{M}-\text{O})_{\text{I}}}$	$d_{(\text{M}-\text{H})_{\text{I}}}$	$d_{(\text{M}-\text{O})_{\text{II}}}$	$d_{(\text{M}-\text{H})_{\text{II}}}$
$[\text{Mg}(\text{H}_2\text{O})_6]^{2+}$	T_h	2.21 (2.00–2.15)	2.90	—	—
$[\text{Mg}(\text{H}_2\text{O})_{18}]^{2+}$	T_h	2.19 (2.07–2.10)	2.89	4.50	4.78, 5.39
	S_6	2.19 (2.10)	2.87 (2.78)	4.13 (4.13)	4.07, 5.04 (5.02)
$[\text{Mg}(\text{H}_2\text{O})_{42}]^{2+}$	T_h	2.20	2.85	4.39	4.61
	S_6	2.22	2.83	4.29	4.40
System	Symmetry	$d_{(\text{M}-\text{O})_{\text{I}}}$	$d_{(\text{M}-\text{H})_{\text{I}}}$	$d_{(\text{M}-\text{O})_{\text{II}}}$	$d_{(\text{M}-\text{H})_{\text{II}}}$
$[\text{Al}(\text{H}_2\text{O})_6]^{3+}$	T_h	2.00 (1.87–1.95)	2.71	—	—
$[\text{Al}(\text{H}_2\text{O})_{18}]^{3+}$	T_h	1.98	2.69	4.22	4.61, 5.07
	S_6	1.98 (1.92)	2.68 (3.99)	4.01	4.10, 4.87
$[\text{Al}(\text{H}_2\text{O})_{42}]^{3+}$	T_h	1.98	2.68	4.28	4.78
	S_6	1.99	2.64	3.93	4.36

1
2
3
4
5
6
7 by one or the other symmetry type.
8

9 The distance between the metal center and the oxygen atoms in the first hydration
10 shell ($M-O_I$) is shortened in the $[M(H_2O)_{18}]^{m+}$ clusters with respect to the $[M(H_2O)_6]^{m+}$
11 structures, since the interaction between water molecules in the first shell with outer water
12 molecules enhances the transfer of electron density towards the metal center.^{22,37} However,
13 further inclusion of a third solvation shell translates into a slight elongation of the $M-O_I$
14 distances, showing that the water–water interactions between the first and second shells
15 are hampered by the presence of a third shell of water molecules.
16
17

18 The $M-O$ and $M-H$ interatomic distances in a $[M(H_2O)_n]^{m+}$ structure are always
19 shorter for Al^{3+} than for Mg^{2+} , since the higher net charge on the metal center in the
20 case of Al makes the metal–water interactions stronger. However, the difference between
21 the $M-O$ distances in the first and second solvation shells ($d_{(M-O)_{II}} - d_{(M-O)_I}$) is very
22 similar for the T_h or S_6 $[M(H_2O)_{18}]^{m+}$ clusters of both Mg^{2+} and Al^{3+} . The polarization
23 experienced by water molecules in the first shell of Al^{3+} is of greater magnitude than for
24 water molecules in the first shell of Mg^{2+} , but this difference does not affect to a great
25 extent the interactions between water molecules in the first and second hydration shells
26 of the ion. Once the first hydration shell of a metal ion is defined, its interaction with
27 the water molecules in the second shell and in the bulk is unspecific with respect to the
28 chemical identity of the ion, but is dominated by the conformation adopted by the first
29 shell.
30
31
32
33
34
35
36
37
38
39
40
41
42
43
44
45
46
47
48
49

50 3.3 Energy analysis 51

52 In order to assess the relative stabilities of the microsolvated clusters considered in this
53 study, we have computed the energy differences between the T_h and S_6 conformers in-
54 cluding two and three hydration shells, which are reported in Table 2. For the case of the
55 two-shell structures, the S_6 conformer is energetically more stable than the T_h one, for
56 both Mg^{2+} and Al^{3+} . The resulting energy differences are in agreement with the values
57 for both Mg^{2+} and Al^{3+} . The resulting energy differences are in agreement with the values
58 for both Mg^{2+} and Al^{3+} . The resulting energy differences are in agreement with the values
59 for both Mg^{2+} and Al^{3+} . The resulting energy differences are in agreement with the values
60 for both Mg^{2+} and Al^{3+} .

previously reported by Markham et al²⁴ for Mg^{2+} (34–41 kcal/mol). However, when a third solvation shell is included in the calculation, the tendency is reversed and the T_h arrangement is clearly favored, recovering the behavior observed for these metal ions in aqueous solution. The energy difference is so large that one would not expect to observe the S_6 conformer even at room temperature.

Table 2: Energy difference (kcal/mol) between the T_h and S_6 conformers with two and three hydration shells, including the metal hexahydrate (ΔE) or excluding it in the calculation of the total energy (ΔE^W).

	$\Delta E(T_h - S_6)$	$\Delta E^W(T_h - S_6)$		$\Delta E(T_h - S_6)$	$\Delta E^W(T_h - S_6)$
$[Mg(H_2O)_{18}]^{2+}$	+44.6	+88.4	$[Al(H_2O)_{18}]^{3+}$	+25.4	+74.3
$[Mg(H_2O)_{42}]^{2+}$	-64.8	-63.2	$[Al(H_2O)_{42}]^{3+}$	-63.6	-39.5

This behavior can be understood in terms of different interaction energy contributions. When the metal is surrounded by only the first hydration shell, the orientation of water molecules is driven by electrostatic interactions with the cation. The most stable arrangement is the one that maximizes the metal–water electrostatic interaction, but minimizes the water–water repulsion. Therefore the T_h conformer is preferred.

When a second shell of water molecules is considered, the S_6 arrangement favors attractive water–water interactions within the second shell, yielding the crown-shaped structure shown in Fig. 1c,d. The energetic gain in terms of water–water interaction is enough to modify the geometrical arrangement of the inner hexahydrate by tilting the water molecules in the first hydration shell. If a third solvation shell is added, the T_h configuration is recovered since this conformation allows a maximum interaction of the $[M(H_2O)_{18}]^{m+}$ unit with the remaining solvent molecules.

In order to illustrate these ideas, we have computed the total energy for the $(H_2O)_{12}$ and $(H_2O)_{36}$ arrangements of water molecules corresponding to the second or second–and–third solvation shells in the $[M(H_2O)_{18}]^{m+}$ and $[M(H_2O)_{42}]^{m+}$ clusters obtained from QM–optimization and annealing, respectively. To this aim the structures and spatial distribution of water molecules in the $(H_2O)_{12}$ and $(H_2O)_{36}$ systems are kept frozen with

1
2
3
4
5
6
7 respect to the structures of the clusters including the metal hexahydrate. The energy
8 differences between the T_h and S_6 arrangements of second-shell $(\text{H}_2\text{O})_{12}$ or second- and
9 third-shell $(\text{H}_2\text{O})_{36}$ water molecules, $\Delta E^W(T_h - S_6)$, are included in Table 2. In the
10 clusters containing a cation surrounded by two solvation shells, $[\text{M}(\text{H}_2\text{O})_{18}]^{m+}$, the water-
11 water interactions are enough to stabilize the S_6 versus the T_h conformers. When a third
12 hydration shell is included, the water-water interactions favor the T_h arrangement of
13 water molecules around the metal ion. This result is in agreement with our picture of
14 a S_6 -crown-shaped second hydration shell in which water molecules interact with each
15 other rather than with water molecules in some outer shell. The presence of a third
16 solvation shell favors the maximization of the water-water interaction through adoption
17 of a T_h -like distribution of water molecules around the metal ion.
18
19

20 An alternative way to consider the solvation effects is via the use of a continuum model
21 instead of explicit water molecules to represent the solvent. In such an approximation one
22 really deals with a cation in solution, whereas in the case of the cluster including three
23 hydration shells the system consists of a multiply-hydrated cation in gas phase, or a drop.
24 We have used the PCM model within the IEFPCM formalism³⁸ to optimize the structures
25 of the $[\text{M}(\text{H}_2\text{O})_{18}]^{m+}$ clusters in the T_h and S_6 arrangements. Contrarily to the results
26 obtained using three explicit hydration shells, the preference for the T_h arrangement is not
27 recovered using the continuum model. A detailed comparative analysis of the importance
28 of using a molecular description of the solvent instead of a continuum representation in
29 order to study the relative stabilities of different conformers is currently being developed
30 in our group for a series of metal cations, and will be the topic of another publication.
31
32
33
34
35
36
37
38
39
40
41
42
43
44
45
46
47
48
49
50
51
52
53

54 **3.4 Analysis of hydrogen bonds**

55
56

57 An additional way to quantify the water-water interactions within the different hydration
58 complexes consists in taking into account the number of hydrogen bonds (HB) established
59 between adjacent hydration shells. We have adopted the criteria used by Chandra³⁹ to
60

define a hydrogen bond between water molecules: the distance between the two oxygen atoms is shorter than 3.5 Å, the distance between the accepting oxygen atom O* and the hydrogen atom is less than 2.45 Å, and the $\widehat{\text{OO}^*\text{H}}$ angle is less than 30°. Then we define three indexes: W_1 is the number of HB per water molecule in which a first-shell water molecule takes part. W_{21} is the number of HB per water molecule established between water molecules in the second shell and water molecules in the first shell. W_{22} is the number of HB per water molecule formed between second-shell water molecules. Table 3 shows the values of these indexes obtained for the optimized $[\text{M}(\text{H}_2\text{O})_{18}]^{m+}$ structures and for the final $[\text{M}(\text{H}_2\text{O})_{42}]^{m+}$ structures obtained from the annealing process. In this sense, the two-shell structures serve as a reference in order to quantify the distortion from the original T_h or S_6 symmetry in the disordered $[\text{M}(\text{H}_2\text{O})_{42}]^{m+}$ structures.

Table 3: Number of hydrogen bonds per water molecule in the microsolvated complexes of Mg and Al including two and three hydration shells.

	T_h			S_6		
	W_1	W_{21}	W_{22}	W_1	W_{21}	W_{22}
$[\text{Mg}(\text{H}_2\text{O})_{18}]^{2+}$	2.00	1.00	0.00	2.00	1.00	1.00
$[\text{Mg}(\text{H}_2\text{O})_{42}]^{2+}$	2.00	0.92	0.23	2.17	0.93	0.57
$[\text{Al}(\text{H}_2\text{O})_{18}]^{3+}$	2.00	1.00	0.00	2.00	1.00	1.00
$[\text{Al}(\text{H}_2\text{O})_{42}]^{3+}$	2.00	1.00	0.00	2.33	1.00	0.71

The W_1 index equals 2.00 for the two-shell structures, since in the symmetric clusters each water molecule in the first shell forms two hydrogen bonds with accepting water molecules in the second-shell. When the water molecules form the crown-shaped S_6 structure, they are distributed within a restricted volume around the metal center, and void regions are defined above and below such crown allowing for water molecules in the second shell to donate HB to first-shell water molecules, W_1 becoming greater than 2.00. This can also happen in the T_h conformer if the M–O distance is long enough, as in the case of Mg^{2+} . However in the present case there is a fortuitous cancellation: the second

1
2
3
4
5
6
7 shell of Mg^{2+} is not so strongly structured as in Al^{3+} , not all first-shell water molecules
8 give 2 HB towards the second shell, and there are also first-shell water molecules accepting
9 HB from the second shell, resulting in W_1 equals 2.00.
10
11

12 W_{21} equals 1.00 for the four two-shells optimized structures, since each second-shell
13 water molecules accepts a HB from a water molecule in the first shell. In the case of
14 the three-shell structures, for Mg^{2+} the second shell is more diffuse, less defined, there
15 are more than 12 water molecules in the second shell and not all of them form HB with
16 first-shell water molecules, resulting in a W_{21} value of less than 1.00. For Al^{3+} the second
17 shell is much better defined and we do not observe a value smaller than 1.00.
18
19

20 The W_{22} index provides a useful and simple way to distinguish between the T_h and S_6
21 coordination modes. In a strictly defined, highly symmetrical T_h arrangement of water
22 molecules, water molecules in the second shell cannot form HB with other second-shell
23 water molecules (see Fig. 1b) and W_{22} is zero. Likewise, in a highly symmetrical S_6
24 arrangement, each second-shell water molecules forms a HB with another water molecules,
25 and W_{22} is 1.00 (see Fig. 1c,d). According to this definition we can observe that in the final
26 structures from the annealing, the symmetry of the starting configuration has remained
27 quite unaffected in spite of the thermal fluctuations. However, the crown-like arrangement
28 of second-shell water molecules in the S_6 conformers at the end of the annealing is slightly
29 distorted towards the much more stable T_h conformation. The distortions from the initial
30 symmetry are higher for Mg^{2+} , given its less defined second hydration shell. The value
31 of W_{22} greater than zero in the T_h Mg^{2+} conformer responds to the fact that there are
32 more than 12 water molecules in the second solvation shell of the metal, and thus there
33 is certain degree on hydrogen bonding within the second shell.
34
35

36 In the absence of thermal agitation, in an ideal hydrogen-bonded structured water,
37 each water molecule in the second shell would ideally form 4 HB in total, one of each would
38 bind it to a water molecule in the first shell, and the other three remaining available for
39 interaction with other water molecules. In a two-shell structure, the second-shell water
40

molecules achieve a higher saturation of their interaction sites by establishing HB with other second-shell water molecules, and the S_6 conformer is more stable. When a third solvation shell is considered, the more stable arrangement is the one that allows a maximum occupation of space through a maximum interaction of second-shell water molecules with other solvent water molecules. That is achieved by adopting a T_h arrangement.

4 Concluding remarks

When an aqua ion composed of a hexahydrated metal cation plus a certain number of additional water molecules distributed within different hydration shells is considered, the energetic enhancement of a T_h versus a S_6 structure, and vice-versa, is intrinsic to the arrangement of water molecules within the second shell and is a function of the degree of hydration, i.e. the number of hydration shells surrounding the metal cation determines the preferred arrangement. There are two contributions taking part: metal cation–water and water–water interactions, the water–water contribution becoming determinant when there are two or more hydration shells included to describe the system. In a structure containing two hydration shells, the key point for the appearance of the S_6 arrangement is joined to the ability of second-shell water molecules to combine their coordination with water molecules in the first shell and water–water interactions within the second shell. This can be achieved if the octahedral disposition of the hexahydrated aqua ion is distorted leading to the S_6 conformer. When a third hydration shell is added, the water molecules in the second shell form new hydrogen bonds with water molecules in the third shell, and the second-shell network is partially lost. Then the T_h conformer is recovered as the preferred conformer. **The use of a molecular description of the solvent in the third solvation shell is mandatory in order to recover the T_h arrangement of water molecules, given that a continuum representation of the solvent is not sufficient to provide the solvent–solvent interactions that reverse the relative stabilities between the S_6 and T_h conformers including only two hydration shells.** Furthermore, the present results show that the use of only

1
2
3
4
5
6
7 two hydration shells are useful to characterize gas-phase microsolvated clusters, but does
8 not warrant a proper description of metal aqua ions in solution. The results presented
9 in this contribution concern isolated molecular aggregates at temperatures close to 0 K.
10 The inclusion of temperature effects and outer solvations shells to achieve the description
11 of a condensed medium will be undertaken in the future.
12
13
14
15
16
17
18
19

Acknowledgements

20
21 This contribution is dedicated to the memory of Dr. José Antonio Mejías, a friendly
22 colleague and enthusiastic scientist. We acknowledge Spanish Ministerio de Ciencia e
23 Innovacion for financial support (CTQ2008-05277). E.C.B. thanks Junta de Andalucía
24 for a postdoctoral fellowship (P06-FQM-01484).
25
26
27
28
29
30
31
32
33
34
35
36
37
38
39
40
41
42
43
44
45
46
47
48
49
50
51
52
53
54
55
56
57
58
59
60

References

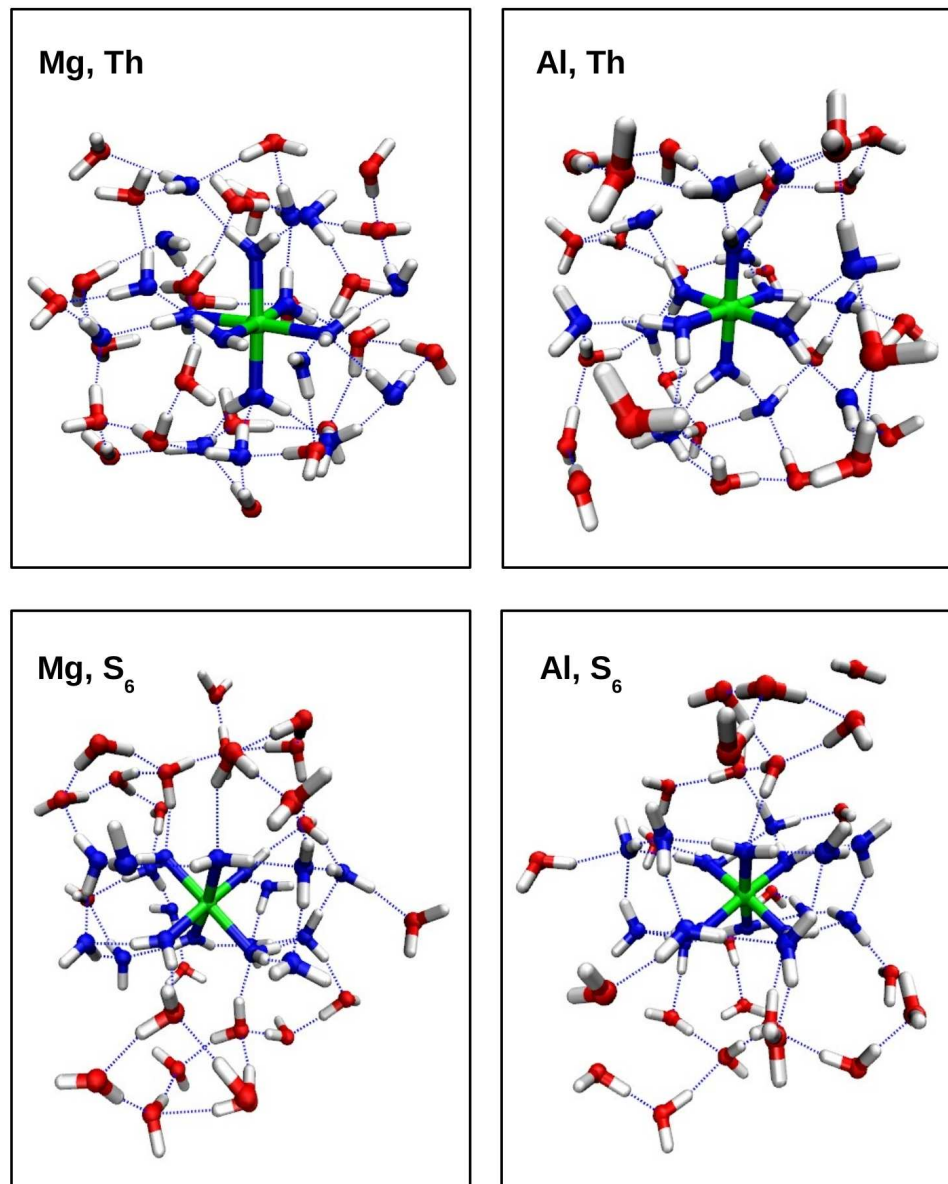
1. Richens, D. T. *The Chemistry of Aqua Ions*; John Wiley: Chichester, 1997.
2. Frank, H. S.; Evans, M. W. *J. Chem. Phys.* **1945**, *13*, 507–532.
3. Ohtaki, H.; Radnai, T. *Chem. Rev.* **1993**, *93*, 1157–1204.
4. Magini, M.; Licheri, G.; G. Paschina, G. P.; Pinna, G. *X-ray Diffraction of Ions in Aqueous Solution: Hydration, and Complex Formation*; CRC: Boca Raton, FL, 1988.
5. Marcus, Y. *Ion Solvation*; Wiley: Chichester, 1986.
6. Enderby, J. E.; Cummings, S.; Herkman, G. J.; Neilson, G. W.; Salmon, P. S.; Skipper, N. *J. Phys. Chem.* **1987**, *91*, 5851–5858.
7. Jayaweera, P.; Blades, A. T.; Ikonomou, M. G.; Kebarle, P. *J. Am. Chem. Soc.* **1990**, *112*, 2452–2454.

- 1
2
3
4
5
6
7 8. Peschke, M.; Blades, A. T.; Kebarle, P. *J. Phys. Chem. A* **1998**, *102*, 9978–9985.
8
9
10 9. Rodriguez-Cruz, S. E.; Jockusch, R. A.; Williams, E. R. *J. Am. Chem. Soc.* **1999**,
11 121, 8898–8906.
12
13
14 10. Robertson, W. H.; Johnson, M. A. *Annu. Rev. Phys. Chem.* **2003**, *54*, 173–213.
15
16
17 11. Bush, M. F.; Saykally, R. J.; Williams, E. R. *J. Am. Chem. Soc.* **2008**, *130*, 9122–
18 9128.
19
20
21 12. Bush, M. F.; Saykally, R. J.; Williams, E. R. *J. Am. Chem. Soc.* **2009**, *131*, in press.
22
23
24 13. Pullman, A. In *Quantum Theory of Chemical Reactivity*; Daudel, R.; Pullman, A.;
25 Salem, L.; Veillard, A., Eds.; Reidel Publish.: Dordrecht, 1980, Vol. 2, Chapter 1.
26
27
28 14. Rivail, J. L.; Rinaldi, D. *Chem. Phys.* **1976**, *18*, 233–242.
29
30
31 15. Miertus, S.; Scrocco, E.; Tomasi, J. *Chem. Phys.* **1981**, *55*, 117–129.
32
33
34 16. Claverie, P.; Daudey, J. P.; Langlet, J.; Pullman, B.; Piazzola, D.; Huron, M. J. *J. Phys. Chem.* **1978**, *82*, 405–418.
35
36
37 17. Sánchez Marcos, E.; Terryn, B.; Rivail, J. L. *J. Phys. Chem.* **1985**, *89*, 4695–4700.
38
39
40 18. Helgaker, T.; Uggerud, E.; Jensen, H. J. A. *Chem. Phys. Lett.* **1990**, *173*, 145–150.
41
42
43 19. Car, R.; Parrinello, M. *Phys. Rev. Lett.* **1985**, *55*, 2471–2474.
44
45
46 20. Burgess, J. *Metal Ions in Solution*; Ellis Horwood: New York, 1978.
47
48
49 21. Bergström, P. A.; Lindgren, J.; Read, M.; Sandström, M. *J. Phys. Chem.* **1991**, *95*,
50 7650–7655.
51
52
53 22. Pavlov, M.; Siegbahn, P. E. M.; Sandström, M. *J. Phys. Chem. A* **1998**, *102*, 219–228.
54
55
56 23. Wasserman, E.; Rustad, J. R.; Xantheas, S. *J. Chem. Phys.* **1997**, *106*, 9769–9780.
57
58
59
60

- 1
2
3
4
5
6
7 24. Markham, G. D.; Glusker, J. P.; Bock, C. W. *J. Phys. Chem.* **2002**, *106*, 5118–5134.
8
9 25. Pye, C. C.; Rudolph, W. W. *J. Phys. Chem. A* **1998**, *102*, 9933–9943.
10
11 26. Bock, C. W.; Markham, G. D.; Katz, A. K.; Glusker, J. P. *Theor. Chem. Acc.* **2006**,
12
13 115, 100–112.
14
15
16 27. Martinez, J. M.; Martinez, L. *J. Comput. Chem.* **2003**, *24*, 819–825.
17
18 28. Martinez, L.; Andrade, E.; Birgin, E. G.; Martinez, L. *J. Comput. Chem.* **2009**, *30*,
19
20 in press.
21
22
23 29. CPMD V3.11, Copyright IBM Corp. 1990-2006, Copyright MPI für
24
25 Festkörperforschung Stuttgart 1997-2001.
26
27
28 30. Troullier, N.; Martins, J. L. *Phys. Rev. B* **1991**, *43*, 1993–2006.
29
30
31 31. Marx, D.; Hutter, J. In *Modern Methods and Algorithms of Quantum Chemistry*;
32
33 Grotendorst, J., Ed., 2nd ed.; NIC, FZ Jülich, 2000, pp 329–477.
34
35
36 32. Perdew, J. P.; Burke, K.; Ernzerhof, M. *Phys. Rev. Lett.* **1996**, *77*, 3865–3868.
37
38 33. Perdew, J. P.; Burke, K.; Ernzerhof, M. *Phys. Rev. Lett.* **1997**, *78*, 1396–1396.
39
40
41 34. Krishnan, R.; Binkley, J. S.; Seeger, R.; Pople, J. A. *J. Chem. Phys.* **1980**, *72*, 650–
42
43 654.
44
45
46 35. McLean, A. D.; Chandler, G. S. *J. Chem. Phys.* **1980**, *72*, 5639–5648.
47
48
49 36. M. J. Frisch *et al.*, *Gaussian 03, Revision C.02*, Gaussian, Inc., Wallingford, CT,
50
51 2004.
52
53
54 37. Martínez, J. M.; Pappalardo, R. R.; Sánchez Marcos, E. *J. Phys. Chem. A* **1997**, *101*,
55
56 4444.
57
58
59 38. Mennucci, B.; Tomasi, J. *J. Chem. Phys.* **1997**, *106*, 5151–5158.
60

- 1
2
3
4
5
6
7 39. Chandra, A. *Phys. Rev. Lett.* **2000**, *85*, 768–771.
8
9
10
11
12
13
14
15
16
17
18
19
20
21
22
23
24
25
26
27
28
29
30
31
32
33
34
35
36
37
38
39
40
41
42
43
44
45
46
47
48
49
50
51
52
53
54
55
56
57
58
59
60

For Peer Review Only



187x232mm (200 x 200 DPI)

1
2
3
4
5
6
7
8
9
10
11
12 Opposite effects of successive hydration shells on the
13
14 aqua ion structure of metal cations
15
16
17
18
19

20 Elizabeth C. Beret, Elsa Galbis, Rafael R. Pappalardo
21
22 and Enrique Sánchez Marcos*
23
24

25 Departamento de Química Física, Universidad de Sevilla,
26
27 41012 Sevilla, Spain. e-mail:sanchez@us.es
28
29

30 April 23, 2009
31
32
33
34
35

36 Supporting Information 37

38
39 Comparison between the structures obtained with plane waves
40
41 and with Gaussian functions.
42
43
44
45
46
47
48
49
50
51
52
53
54
55
56
57
58
59
60

1 2 3 4 5 6 7 8 9 10 11 12 13 14 15 16 17 18 19 20 21 22 23 24 25 26 27 28 29 30 31 32 33 34 35 36 37 38 39 40 41 42 43 44 45 46 47 48 49 50 51 52 53 54 55 56 57 58 59 60

Table 1: Comparison between the structures obtained with plane waves (*p.w.*) and Gaussian functions (*g.f.*) for the solvation complexes of Mg^{2+} and Al^{3+} including a different number of hydration shells (distances in Å and angles in sexagesimal degrees).

System	Symmetry	$d_{(M-O)_I}$	$d_{(M-H)_I}$	$d_{(O-H)_I}$	$\alpha_{(H-O-H)_I}$	$\alpha_{(O-M-O)_I}$	$d_{(M-O)_{II}}$	$d_{(M-H)_{II}}$	$d_{(O-H)_{II}}$	$d_{(M-O-H)_{II}}$	$\alpha_{(H-O-H)_{II}}$
		<i>g.f.</i>	<i>p.w.</i>	<i>g.f.</i>	<i>p.w.</i>	<i>g.f.</i>	<i>p.w.</i>	<i>g.f.</i>	<i>p.w.</i>	<i>g.f.</i>	<i>p.w.</i>
$[Mg(H_2O)_6]^{2+}$	T_h	2.11	2.21	2.81	2.90	0.97	0.98	106.4	105.5	90.0	90.0
		2.10	2.19	2.78	2.87	0.98	0.99	109.6	109.0	89.0, 91.0	89.9, 90.1
$[Mg(H_2O)_{18}]^{2+}$	T_h	2.09	2.19	2.79	2.89	0.98	0.99	108.1	106.2	90.0	90.0
		2.10	2.19	2.78	2.87	0.98	0.99	109.6	109.0	89.0, 91.0	89.9, 90.1
$[Al(H_2O)_6]^{3+}$	T_h	1.94	2.00	2.64	2.71	0.98	0.99	107.5	106.9	90.0	90.0
		1.92	1.98	2.63	2.69	1.00	1.01	109.1	108.6	90.0	90.0
$[Al(H_2O)_{18}]^{3+}$	S_6	1.92	1.98	2.62	2.67	1.00	1.01	110.0	110.3	89.4, 90.6	89.2, 90.8
		1.92	1.98	2.62	2.67	1.00	1.01	110.0	110.3	89.4, 90.6	89.2, 90.8

1
2
3
4
5
6
7 Coordinates of the optimized $[\text{Mg}(\text{H}_2\text{O})_{18}]^{2+}$ cluster in T_h sym-
8
9 metry.

10 55

13	Mg	0.000000	0.000000	0.000000
14	O	0.000000	0.000000	-2.093442
15	O	0.000000	2.093442	0.000000
16	O	0.000000	-2.093442	0.000000
17	O	-2.093442	0.000000	0.000000
18	O	2.093442	0.000000	0.000000
19	O	0.000000	0.000000	2.093442
20	H	0.796496	0.000000	-2.670690
21	H	-0.796496	0.000000	-2.670690
22	H	0.796496	0.000000	2.670690
23	H	0.000000	2.670690	0.796496
24	H	0.000000	-2.670690	-0.796496
25	H	0.000000	-2.670690	0.796496
26	H	0.000000	2.670690	-0.796496
27	H	0.000000	2.670690	-0.796496
28	H	-2.670690	0.796496	0.000000
29	H	2.670690	-0.796496	0.000000
30	H	2.670690	0.796496	0.000000
31	H	-2.670690	-0.796496	0.000000
32	H	-0.796496	0.000000	2.670690
33	O	0.000000	3.706130	2.261862
34	O	0.000000	-3.706130	2.261862
35	O	0.000000	-3.706130	-2.261862
36	O	-3.706130	-2.261862	0.000000
37	O	-3.706130	2.261862	0.000000
38	O	3.706130	2.261862	0.000000
39	O	3.706130	-2.261862	0.000000
40	O	2.261862	0.000000	3.706130
41	O	-2.261862	0.000000	3.706130
42	O	-2.261862	0.000000	-3.706130
43	O	2.261862	0.000000	-3.706130
44	O	0.000000	3.706130	-2.261862
45	H	0.000000	3.290752	3.137853
46	H	0.000000	-3.290752	3.137853
47	H	0.000000	-3.290752	-3.137853
48	H	0.000000	3.290752	-3.137853
49	H	-3.290752	-3.137853	0.000000
50	H	-3.290752	3.137853	0.000000
51	H	3.290752	3.137853	0.000000
52	H	3.290752	-3.137853	0.000000
53	H	3.137853	0.000000	3.290752
54	H	-3.137853	0.000000	3.290752
55	H	-3.137853	0.000000	-3.290752
56	H	3.137853	0.000000	-3.290752
57	H	0.000000	3.290752	-3.137853
58	H	0.000000	4.661980	2.424881
59	H	0.000000	-4.661980	2.424881
60	H	0.000000	-4.661980	-2.424881
	H	-4.661980	-2.424881	0.000000

```

1
2
3
4
5
6
7     H    -4.661980    2.424881    0.000000
8     H     4.661980    2.424881    0.000000
9     H     4.661980   -2.424881    0.000000
10    H     2.424881    0.000000    4.661980
11    H    -2.424881    0.000000    4.661980
12    H    -2.424881    0.000000   -4.661980
13    H     2.424881    0.000000   -4.661980
14    H     0.000000    4.661980   -2.424881
15
16
17 Coordinates of the optimized  $[\text{Mg}(\text{H}_2\text{O})_{18}]^{2+}$  cluster in  $S_6$  sym-
18 metry.
19
20      55
21
22
23
24
25
26
27
28
29
30
31
32
33
34
35
36
37
38
39
40
41
42
43
44
45
46
47
48
49
50
51
52
53
54
55
56
57
58
59
60

```

Coordinates of the optimized $[\text{Mg}(\text{H}_2\text{O})_{18}]^{2+}$ cluster in S_6 symmetry.

22	Mg	0.000000	0.000000
23	O	-1.091370	1.341721
24	O	-0.616279	-1.616015
25	O	0.616279	1.616015
26	O	-1.707650	-0.274294
27	O	1.091370	-1.341721
28	O	1.707650	0.274294
29	H	-0.794481	2.246247
30	H	-1.548067	-1.811164
31	H	1.548067	1.811164
32	H	-2.342548	0.435083
33	H	0.794481	-2.246247
34	H	2.342548	-0.435083
35	H	-2.044444	1.245917
36	H	-0.056773	-2.393499
37	H	0.056773	2.393499
38	H	-2.101218	-1.147582
39	H	2.044444	1.245917
40	H	2.101218	1.147582
41	O	-3.835701	0.807990
42	O	1.218111	-3.725810
43	O	-1.218111	3.725810
44	O	-2.617591	-2.917820
45	O	3.835701	-0.807990
46	O	2.617591	2.917820
47	H	-3.829665	-0.183631
48	H	2.073862	-3.224771
49	H	-2.073862	3.224771
50	H	-1.755803	-3.408402
51	H	3.829665	0.183631
52	H	1.755803	3.408402
53	H	-4.494373	1.067727
54	H	1.322508	-4.426105
55	H	-1.322508	4.426105
56	H	-3.171865	-3.358378
57	H	4.494373	-1.067727
58	H	3.171865	3.358378
59	O	0.000000	3.922236
60			1.227865

1
 2
 3
 4
 5
 6
 7 O -3.396756 -1.961118 1.227865
 8 O 3.396756 1.961118 -1.227865
 9 O -3.396756 1.961118 -1.227865
 10 O 0.000000 -3.922236 -1.227865
 11 O 3.396756 -1.961118 1.227865
 12 H -0.438140 4.082511 0.353422
 13 H -3.316488 -2.420696 0.353422
 14 H 3.316488 2.420696 -0.353422
 15 H -3.754628 1.661815 -0.353422
 16 H 0.438140 -4.082511 -0.353422
 17 H 3.754628 -1.661815 0.353422
 18 H -0.241028 4.671012 1.798031
 19 H -3.924701 -2.544242 1.798031
 20 H 3.924701 2.544242 -1.798031
 21 H -4.165729 2.126769 -1.798031
 22 H 0.241028 -4.671012 -1.798031
 23 H 4.165729 -2.126769 1.798031
 24

25
 26 Coordinates of the optimized $[Al(H_2O)_{18}]^{3+}$ cluster in T_h symme-
 27 try.
 28

29 55
 30
 31
 32 Al 0.000000 0.000000 0.000000
 33 O 0.000000 0.000000 -1.915848
 34 O 0.000000 1.915848 0.000000
 35 O 0.000000 -1.915848 0.000000
 36 O -1.915848 0.000000 0.000000
 37 O 1.915848 0.000000 0.000000
 38 O 0.000000 0.000000 1.915848
 39 H 0.815740 0.000000 -2.496533
 40 H -0.815740 0.000000 -2.496533
 41 H 0.815740 0.000000 2.496533
 42 H 0.000000 2.496533 0.815740
 43 H 0.000000 -2.496533 -0.815740
 44 H 0.000000 -2.496533 0.815740
 45 H 0.000000 2.496533 -0.815740
 46 H -2.496533 0.815740 0.000000
 47 H 2.496533 -0.815740 0.000000
 48 H 2.496533 0.815740 0.000000
 49 H -2.496533 -0.815740 0.000000
 50 H -0.815740 0.000000 2.496533
 51 O 0.000000 3.595497 2.071728
 52 O 0.000000 -3.595497 2.071728
 53 O 0.000000 -3.595497 -2.071728
 54 O -3.595497 -2.071728 0.000000
 55 O -3.595497 2.071728 0.000000
 56 O 3.595497 2.071728 0.000000
 57 O 3.595497 -2.071728 0.000000
 58 O 2.071728 0.000000 3.595497
 59 O -2.071728 0.000000 3.595497
 60 O -2.071728 0.000000 -3.595497

1
 2
 3
 4
 5
 6
 7 O 2.071728 0.000000 -3.595497
 8 O 0.000000 3.595497 -2.071728
 9 H 0.000000 3.380682 3.017778
 10 H 0.000000 -3.380682 3.017778
 11 H 0.000000 -3.380682 -3.017778
 12 H -3.380682 -3.017778 0.000000
 13 H -3.380682 3.017778 0.000000
 14 H 3.380682 3.017778 0.000000
 15 H 3.380682 -3.017778 0.000000
 16 H 3.017778 0.000000 3.380682
 17 H -3.017778 0.000000 3.380682
 18 H -3.017778 0.000000 -3.380682
 19 H 3.017778 0.000000 -3.380682
 20 H 0.000000 3.380682 -3.017778
 21 H 0.000000 4.565566 2.025984
 22 H 0.000000 -4.565566 2.025984
 23 H 0.000000 -4.565566 -2.025984
 24 H -4.565566 -2.025984 0.000000
 25 H -4.565566 2.025984 0.000000
 26 H 4.565566 2.025984 0.000000
 27 H 4.565566 -2.025984 0.000000
 28 H 2.025984 0.000000 4.565566
 29 H -2.025984 0.000000 4.565566
 30 H -2.025984 0.000000 -4.565566
 31 H 2.025984 0.000000 -4.565566
 32 H 0.000000 4.565566 -2.025984
 33 H 0.000000 4.565566 2.025984
 34
 35
 36 Coordinates of the optimized $[Al(H_2O)_{18}]^{3+}$ cluster in S_6 symme-
 37 try.
 38
 39 55
 40
 41 Al 0.000000 0.000000 0.000000
 42 O -1.367729 -0.789658 1.098471
 43 O 1.367729 -0.789658 1.098471
 44 O -1.367729 0.789658 -1.098471
 45 O 0.000000 -1.579317 -1.098471
 46 O 1.367729 0.789658 -1.098471
 47 O 0.000000 1.579317 1.098471
 48 H -2.234175 -0.339993 1.319899
 49 H 1.411531 -1.764856 1.319899
 50 H -1.411531 1.764856 -1.319899
 51 H -0.822645 -2.104849 -1.319899
 52 H 2.234175 0.339993 -1.319899
 53 H 0.822645 2.104849 1.319899
 54 H -1.431563 -1.771702 1.294514
 55 H 2.250121 -0.353919 1.294514
 56 H -2.250121 0.353919 -1.294514
 57 H 0.818557 -2.125621 -1.294514
 58 H 1.431563 1.771702 -1.294514
 59 H -0.818557 2.125621 1.294514
 60 O -1.454095 -3.456185 1.306924

1
 2
 3
 4
 5
 6
 7 0 3.720191 0.468809 1.306924
 8 0 -3.720191 -0.468809 -1.306924
 9 0 2.266096 -2.987375 -1.306924
 10 0 1.454095 3.456185 -1.306924
 11 0 -2.266096 2.987375 1.306924
 12 H -0.508404 -3.732017 1.370503
 13 H 3.486223 1.425718 1.370503
 14 H -3.486223 -1.425718 -1.370503
 15 H 2.977819 -2.306299 -1.370503
 16 H 0.508404 3.732017 -1.370503
 17 H -2.977819 2.306299 1.370503
 18 H -1.927569 -3.943114 2.005239
 19 H 4.378621 0.302233 2.005239
 20 H -4.378621 -0.302233 -2.005239
 21 H 2.451052 -3.640881 -2.005239
 22 H 1.927569 3.943114 -2.005239
 23 H -2.451052 3.640881 2.005239
 24 O -3.700792 0.525371 1.342533
 25 O 1.395411 -3.467665 1.342533
 26 O -1.395411 3.467665 -1.342533
 27 O -2.305381 -2.942294 -1.342533
 28 O 3.700792 -0.525371 -1.342533
 29 O 2.305381 2.942294 1.342533
 30 H -4.102257 0.220145 0.496191
 31 H 1.860478 -3.662731 0.496191
 32 H -1.860478 3.662731 -0.496191
 33 H -2.241779 -3.442586 -0.496191
 34 H 4.102257 -0.220145 -0.496191
 35 H 2.241779 3.442586 0.496191
 36 H -4.364646 0.365466 2.037783
 37 H 1.865820 -3.962627 2.037783
 38 H -1.865820 3.962627 -2.037783
 39 H -2.498826 -3.597161 -2.037783
 40 H 4.364646 -0.365466 -2.037783
 41 H 2.498826 3.597161 2.037783
 42
 43

44
 45 Coordinates of the $[\text{Mg}(\text{H}_2\text{O})_{42}]^{2+}$ cluster in T_h symmetry after
 46 annealing.
 47

48 127
 49

50
 51 Mg 11.915601507325 12.005157068593 11.416553119413
 52 O 9.144492569943 13.806969884367 8.422768025689
 53 O 12.379249673023 6.662285029345 9.703556823750
 54 O 9.216093859130 9.385016712044 7.739896683975
 55 O 10.296483153976 16.815602747779 14.487812770594
 56 O 10.346273782535 7.478369663059 14.088450230459
 57 O 13.667541152015 13.395817327791 15.546616947150
 58 O 8.861714870999 9.179914300881 10.456477782115
 59 O 10.584370681898 11.995122842653 17.546216993107
 60 O 13.916168097596 11.426280419463 6.928454969181
 O 13.290540826192 16.363369566140 10.050719310688

1				
2				
3				
4				
5				
6				
7	0	14.137878256586	7.391318557198	14.640403535543
8	0	17.051015043486	12.052530882899	16.113404806590
9	0	16.768425246608	9.840062691980	13.101142241874
10	0	16.525668523235	14.944854349391	12.098057772826
11	0	9.413024390269	16.397544610390	8.948322440113
12	0	13.091812813217	11.062497373608	16.910505246342
13	0	16.797832569722	9.979744792158	9.405169148754
14	0	14.996961190207	7.776089991077	9.833932280613
15	0	6.614795480582	10.309931366844	11.484285183590
16	0	15.701166935502	15.529962424766	9.187041799867
17	0	7.152553706812	15.049846097669	12.348379655855
18	0	8.455269418323	9.066454286639	15.343093045910
19	0	13.522870782043	16.997360031908	14.978864993741
20	0	7.545979076727	13.842709367144	14.795980964708
21	0	11.567142558127	12.463919140676	9.262680841826
22	0	14.025787421511	12.507093675328	11.377766582325
23	0	9.765297573409	11.566933986625	11.619454358281
24	0	11.595876456238	14.074786369008	12.087082107049
25	0	12.317523759811	9.922706367832	10.864913187350
26	0	12.148449089305	11.534914128342	13.541972714472
27	0	16.009389952604	12.474396280508	13.376567084845
28	0	8.034940128295	11.262299549442	13.709941883011
29	0	7.759770445621	13.028393087911	10.535782715902
30	0	9.543070065178	16.488693595163	11.791468804145
31	0	13.800768935561	15.628767980521	12.600256493720
32	0	14.402532469230	8.665584002566	12.251534585095
33	0	10.138783380960	6.914481007115	11.415875235197
34	0	12.247395896137	9.263765786558	14.939204323980
35	0	11.206681227425	14.515622005487	15.848026353886
36	0	12.318912445949	14.656138895204	8.194941931519
37	0	12.026295861728	9.600805257955	7.841424507325
38	0	15.468692249419	12.462370669953	9.031027643550
39	H	9.981268999754	13.318476208501	8.625463812787
40	H	9.345837661202	14.785802810443	8.592291488629
41	H	13.206431284080	7.189244789010	9.554995372090
42	H	11.913108355207	6.575651319240	8.824573166354
43	H	8.818619400612	8.539328911224	7.396446243568
44	H	9.062880339899	9.320268583244	8.731856763168
45	H	10.112600813868	16.633660223784	13.523709427583
46	H	9.392496657550	16.948711095126	14.879223198505
47	H	10.515325056868	6.555716233362	14.402870891496
48	H	11.052628754625	8.069425905348	14.479787179211
49	H	13.722470896489	13.091416820933	14.616508835054
50	H	12.789465618409	13.885192503237	15.602403800456
51	H	9.399485213873	9.914362399565	10.855654616370
52	H	9.282532589542	8.329828370513	10.784428992704
53	H	9.984330645429	12.587982312732	18.093567872202
54	H	10.661334233331	12.523577569476	16.722911712968
55	H	13.517139020881	12.030459283538	6.273343722783
56	H	13.182825704900	10.789533337384	7.177303210226
57	H	13.393857071435	16.208902128664	11.033945025120
58	H	12.992925181001	17.316643565713	9.944892429160
59	H	13.853476967229	6.435682173533	14.705859090837

1	H	14.677086139401	7.525418849376	15.475289224426
2	H	16.504702124652	11.393759883355	16.641336316648
3	H	17.728437185293	11.500474352045	15.675688453422
4	H	17.569557209060	9.794792724535	12.496337426455
5	H	17.005693245475	9.345100767610	13.908925443181
6	H	16.452980743808	13.998564254757	12.395013715870
7	H	16.375052499629	14.957094731517	11.121914312337
8	H	9.559713335790	16.426198636364	9.930074409834
9	H	8.459465297423	16.699898585723	8.817202904212
10	H	13.336733541596	11.896440375675	16.407634221706
11	H	12.335908609347	11.357021333492	17.480662312454
12	H	16.426705444837	10.884968577076	9.234205323662
13	H	17.461925083324	10.110379256435	10.122968425815
14	H	14.814191366474	7.939828004183	10.811572290558
15	H	15.514188414372	8.586891810037	9.596160967488
16	H	7.043279118476	10.743282567740	12.276280279446
17	H	7.347281522179	9.726163968969	11.119605589805
18	H	14.814572386910	15.863381544122	9.536873453534
19	H	16.190635436116	16.385021553905	9.033904709571
20	H	7.318441021450	14.334875375846	11.671241278141
21	H	6.171017928047	15.203906209151	12.287121268480
22	H	9.030771765826	8.431594534573	14.830479767605
23	H	8.967714203855	9.228032146097	16.190013726688
24	H	12.623428392986	16.816914742399	15.318575850837
25	H	14.169557722048	16.524831434051	15.591689654589
26	H	7.428663998024	14.310775346822	13.909986416558
27	H	8.434601969644	14.108402446537	15.107223956513
28	H	11.749318838874	11.705185259014	8.671785700805
29	H	11.998581719276	13.299198393327	8.816840477773
30	H	12.225216727163	10.615762629961	13.961196905904
31	H	14.641044481121	12.465335946813	12.150740753321
32	H	9.092270853721	12.151255910326	11.150722848688
33	H	9.323626823637	11.431389946377	12.508401896412
34	H	14.575691179150	12.465009974052	10.549056355402
35	H	12.430692931211	14.595545304608	12.273842572971
36	H	12.342335404221	9.604398262796	9.934070044650
37	H	13.054307419787	9.461556749512	11.354744142491
38	H	10.906894927021	14.738351956913	11.875011206128
39	H	11.493618389034	12.010860699089	14.085567800020
40	H	16.170982704906	12.607660053668	14.342454368274
41	H	7.837197453110	12.109668570315	14.194681004594
42	H	8.132785739625	13.305838728642	9.635782549574
43	H	8.591357919319	16.245207678655	11.948397809860
44	H	14.765362815017	15.393455879371	12.521611812468
45	H	15.227097682557	9.179019832798	12.466870995371
46	H	10.356165256014	7.211944912696	12.345683951675
47	H	12.992252781593	8.590549695623	14.834852110658
48	H	10.897622578939	15.196763690556	15.191406235117
49	H	12.573752880362	15.282688680115	8.935911743627
50	H	12.440811976263	8.844341507049	7.353883978109
51	H	14.855294202962	12.251874860496	8.277733162276
52	H	16.333445518977	11.539649671330	13.242977855641
53	H	8.192280242640	10.534389089951	14.380751402607

1	H	7.114956160941	12.302572990380	10.401182050890
2	H	9.617722443672	17.484450926806	11.659397135140
3	H	13.712903172834	16.171717568536	13.433894368508
4	H	14.291226308182	8.093584030580	13.063736787866
5	H	10.998587967501	6.910995393927	10.912426663160
6	H	12.463284062174	9.768707582984	15.771380722987
7	H	11.123479904995	15.022818573680	16.703913818914
8	H	13.089081902582	14.709032987427	7.565729777054
9	H	11.039667823180	9.497808364549	7.691346744497
10	H	15.735166240446	13.404111354404	8.920126915425

Coordinates of the $[\text{Mg}(\text{H}_2\text{O})_{42}]^{2+}$ cluster in S_6 symmetry after annealing.

127

Mg	11.875472988238	12.042543535400	12.114052818261
O	10.325715439646	10.528773617097	17.588379974518
O	15.599004724176	12.714374165387	7.287385715682
O	12.396962611582	15.701100938136	8.469400283590
O	11.184445394734	7.873798704809	7.768912994317
O	14.840807959566	15.215951223970	7.456145944900
O	7.723446246474	14.747220818835	16.474890637340
O	10.971031534090	12.083573075101	7.676693034955
O	13.599804019454	10.177237616932	4.204650101056
O	12.088052037421	13.601178674475	18.133818827083
O	7.382504116480	11.563494664589	8.148838776874
O	18.229714651685	14.058207539338	13.602878880354
O	14.704048321568	10.158284551957	17.246416332692
O	9.149634533140	12.953200343876	18.132919714441
O	8.802159756555	13.831878795346	7.287062868086
O	11.624318983098	5.747452987635	14.454670132574
O	11.449113623626	16.084644569405	17.204235182436
O	7.738612175051	8.624679525980	11.188967426503
O	13.232947515592	17.422501717670	10.356129778345
O	9.369290724349	9.960275896169	7.077040640021
O	12.585623837625	11.602969787048	16.449593044133
O	11.306057356716	6.402090075232	11.827060353380
O	16.739266584648	11.424651732597	16.048850804632
O	15.896094798994	11.773871711427	9.760848874989
O	13.469946989106	11.160849281076	6.757867811162
O	11.550484779827	10.161922326578	13.147721126964
O	13.062719083809	12.692893642465	13.919416026322
O	10.687333696404	11.359334753499	10.368422471881
O	13.605755730331	11.098255407445	11.118958198767
O	11.973926052810	13.993020842356	10.989286915151
O	10.190048034425	13.044762224490	13.136764228948
O	14.031511578762	9.096091320207	13.775794713512
O	13.380306778623	15.455023712880	14.207446409301
O	10.343984926242	8.599272817575	10.288420584026
O	16.280140691530	13.429928560158	11.768186821021
O	9.137608376307	15.322346259214	11.080510751314

1	O	7.686367038832	11.976666145011	12.896255934832
2	O	8.859912868089	9.686316616105	13.563384438462
3	O	15.443306086804	11.494582084090	13.672028735069
4	O	8.376724876721	12.671883732965	10.460164408797
5	O	15.265284954664	8.475490820662	11.523965694255
6	O	14.197041222069	15.279722758313	11.663011384554
7	O	9.966986942081	15.164309073557	15.029686041638
8	H	9.702053145879	9.962800394383	17.005600916413
9	H	10.564759301068	9.938172401529	18.328338850956
10	H	15.762878780467	12.432592263906	8.244392695058
11	H	14.792561422960	12.164104640560	7.037754295746
12	H	12.669892710227	16.348082626935	9.193129375406
13	H	12.035733617413	14.930212489004	8.962460368810
14	H	10.913780228160	8.105542373198	8.707834075843
15	H	10.975903344386	6.887748740152	7.682969381931
16	H	13.901483502701	15.284064653053	7.809167791964
17	H	15.105307512901	14.234100663065	7.439403859176
18	H	8.205292658422	14.180260822482	17.130542236717
19	H	6.797354494562	14.372119564644	16.433374141894
20	H	11.031102811607	11.875879757380	8.651463826363
21	H	11.875112617947	11.895854885257	7.304721736681
22	H	14.279656013166	9.807671393993	3.524993128187
23	H	13.018693003010	10.764906619293	3.685190691733
24	H	11.133429927288	13.394072185307	18.260524858360
25	H	12.393675873434	12.903532199090	17.468806402372
26	H	8.095170117426	10.906682043686	7.915758260982
27	H	6.563128001309	10.987041957622	8.300647771788
28	H	18.764875811795	14.870350399160	13.379882878636
29	H	17.847355408825	14.218486081384	14.495067741581
30	H	13.869930649346	10.626198602795	16.938329587410
31	H	14.729729299144	9.271347453860	16.789444305327
32	H	9.590073052552	12.056945481311	18.070217238742
33	H	9.226600321402	13.361177167383	19.047522351540
34	H	9.684592510653	13.370802228668	7.327324097918
35	H	8.164243944452	13.135898657273	7.584255920824
36	H	12.393166788391	5.970106092629	15.025202314286
37	H	10.833424903192	6.080760668461	14.984274535992
38	H	11.782090118579	15.189563576539	17.509587222698
39	H	10.915010792370	15.853122242201	16.390328316482
40	H	7.423455328503	9.547220827090	11.129340522807
41	H	7.071813383989	8.101381557643	10.655412588086
42	H	12.541501547501	17.904814797700	10.900288747455
43	H	13.833235750497	18.121002713835	9.978373415465
44	H	10.018884145937	10.724158470529	7.145465897129
45	H	9.895284449168	9.150793524377	7.307763656790
46	H	11.731194922929	11.131545122152	16.660603661378
47	H	12.575591160611	11.893719383824	15.495306130686
48	H	10.529767615251	5.833149860954	11.657335626078
49	H	11.492884952184	6.272673956606	12.808653332515
50	H	17.443813549465	10.756141637132	16.273050190510
51	H	15.940897518732	11.044839755184	16.536421607971
52	H	16.548020829137	11.053543426130	9.547197909518
53	H	16.276764732108	12.384983960791	10.458089985085

1	H	13.595053009170	10.349903676547	7.321617118082
2	H	13.536326171653	10.825591089407	5.822128461186
3	H	10.639317561702	9.843819244898	13.386431844463
4	H	14.003858184629	12.325562689240	13.886269351652
5	H	9.765424660229	11.774760219901	10.400824476506
6	H	13.797898906385	10.143668591854	11.232799111458
7	H	12.791030009656	14.535490526561	11.240066878631
8	H	10.212055538898	13.731081853467	13.849842860898
9	H	12.257983886591	9.592080931739	13.538005882469
10	H	13.143330179493	13.668571684883	14.107692663094
11	H	10.575785547142	10.364547694062	10.365743415155
12	H	14.374078152511	11.409089292584	10.562340835070
13	H	11.176184886177	14.527259916267	11.212705769510
14	H	9.259656899048	12.685684100301	13.134733852710
15	H	14.549190370745	9.946950773720	13.794538763170
16	H	12.662957422856	16.111209432054	14.354913586195
17	H	10.792912682607	8.025655467034	10.960551003982
18	H	15.588045795320	14.145474992491	11.708274842224
19	H	8.844009794253	14.386473540529	10.894479108841
20	H	7.917497122280	11.100570881532	13.325624725340
21	H	14.370195069221	8.549392962316	14.542143559901
22	H	14.166833378017	15.751403495852	14.758415455038
23	H	9.373865880027	8.535853246366	10.521291693886
24	H	17.009698557357	13.774714308400	12.356372189856
25	H	8.929452221875	15.782716190442	10.212817611656
26	H	7.017256028086	12.507532013548	13.396211203356
27	H	8.459383129662	8.984662908992	13.001573806773
28	H	15.813998086910	12.078863306745	12.956454542690
29	H	7.933139404909	12.355445762465	11.301240798501
30	H	14.798722921338	8.531070635157	12.418275726845
31	H	13.965447294121	15.454312532686	12.624795299934
32	H	9.796033683190	15.913555228387	14.426285224540
33	H	8.738632624129	9.415403718005	14.532957991351
34	H	16.066922722061	11.514323663894	14.456459044099
35	H	7.858627617800	12.328070510242	9.680688122306
36	H	16.062657969282	9.025036847339	11.636086930213
37	H	14.034921395727	16.153781958136	11.202860577766
38	H	9.072192497148	14.951375007902	15.433393068284

Coordinates of the $[Al(H_2O)_{42}]^{3+}$ cluster in T_h symmetry after annealing.

127

A1	12.011878405780	12.142974248187	12.093336669141
O	8.766204523131	16.431585098525	9.805095014554
O	12.332343179370	6.862749862701	10.517116930038
O	11.031953465084	13.329944996934	6.132319968374
O	11.054813360007	16.960562534926	15.486586710840
O	9.869144891451	10.626519766611	17.261762818107
O	14.406674280840	12.087667624453	16.587401036169
O	9.480989605798	10.289924298158	8.270461318282

1				
2				
3				
4				
5				
6				
7	0	9.381732977335	8.420789144978	13.799237804116
8	0	13.618961702006	12.617857017499	5.365124625241
9	0	17.923609711085	15.049855812613	12.954930062282
10	0	11.846626838482	7.289226232496	14.845828198161
11	0	15.944166184332	9.096494069087	13.233537730882
12	0	14.088898539559	8.427186326733	16.775137874801
13	0	16.118205776513	15.053164999708	10.822160929770
14	0	11.396251255057	16.558650282770	10.440882186056
15	0	9.750086253329	13.329273611487	17.309928646402
16	0	14.693915755104	11.592040861800	7.667070788387
17	0	13.130500702955	7.614097096285	8.059950797867
18	0	7.840337096383	8.312940340622	9.039862026733
19	0	18.053358685815	11.158057625769	9.685363759834
20	0	7.904707887761	16.504246964038	12.374631582211
21	0	6.650879298254	9.026995777020	11.335307778008
22	0	16.131265413363	16.857258086767	14.306526353074
23	0	6.101798813752	12.585837649368	14.258460857456
24	0	12.121521708163	12.163478813831	10.118916763591
25	0	13.994832496961	12.008300564983	12.186526799237
26	0	10.018526178865	12.296475673664	11.942912915074
27	0	12.120901957088	14.095170854783	12.116558242968
28	0	11.881303642130	10.197563030644	12.044759325830
29	0	11.865038779351	12.171102312649	14.057633189207
30	0	15.737574876059	11.578758944865	14.220778271777
31	0	8.112607440722	10.885530879008	13.279969387976
32	0	8.415405827447	12.297994553612	9.688921392597
33	0	10.467440566760	15.918943767832	12.929329632975
34	0	14.192461793535	15.828669046273	12.462366846179
35	0	13.397096066917	8.139719194089	12.717409943501
36	0	10.111061216071	8.367050924906	11.169752660101
37	0	12.240845899380	10.464300337081	15.961323591126
38	0	11.799615540623	14.297084803310	15.878647383493
39	0	12.097664205857	14.238795295220	8.512659769909
40	0	12.373850606897	10.117811016793	8.182347409355
41	0	15.650299227451	12.484760242934	10.099205364672
42	H	9.751817874976	16.461421805524	9.984882920631
43	H	8.334408862660	16.500291872664	10.712948409056
44	H	12.070363182226	5.900170467879	10.453651146480
45	H	11.473534288258	7.335534634200	10.711677445611
46	H	10.565679849461	12.464172117424	5.945641923647
47	H	10.598716382555	14.013156299922	5.543333918493
48	H	11.419561500728	17.849967563290	15.202834921733
49	H	10.116716724963	17.157183727582	15.792821181993
50	H	9.813578301232	11.630821384521	17.349164970641
51	H	9.139261685646	10.399545262810	16.654598532601
52	H	13.517780628136	11.692867537677	16.377163073267
53	H	14.691389534218	11.491227771192	17.352134100210
54	H	9.135725038645	11.094794766768	8.775590714533
55	H	10.409958738310	10.145906413087	8.566719195296
56	H	10.223921318566	8.248714450498	14.296070101168
57	H	9.110451609137	9.368558211284	13.903329874368
58	H	12.707595447012	12.968577400488	5.572450076099
59	H	14.240267824756	13.395676551348	5.274575923715

1			
2			
3			
4			
5			
6			
7	H	17.349978001595	15.642229034275
8	H	17.401612048146	14.984660197234
9	H	12.476958868654	7.499389910251
10	H	12.327513650394	7.591445665167
11	H	16.485625576145	9.253637950932
12	H	15.872312858982	10.012800134589
13	H	14.421544838728	9.116718981228
14	H	14.800456237164	8.360456785720
15	H	15.946797986437	14.133242096493
16	H	16.152466105983	15.664522773940
17	H	11.740811338001	15.747452595982
18	H	11.174391801182	16.323715744389
19	H	9.846955657490	13.708673227647
20	H	10.513130888527	13.720402067218
21	H	14.307530449910	12.019940988274
22	H	13.996444109791	10.932147196281
23	H	14.119541236429	7.533936747533
24	H	12.812917408608	7.270849925905
25	H	8.461574397124	9.013972250508
26	H	8.105465734163	7.418669040323
27	H	18.131889155231	10.342202808659
28	H	17.885727492769	10.868896390801
29	H	7.122065640978	15.907628340406
30	H	7.704155040588	17.356855163492
31	H	7.106257920205	8.662361848267
32	H	6.461404406411	8.238229224187
33	H	15.381691594132	16.590838854044
34	H	15.813776656669	16.630360909343
35	H	5.994020855192	13.434007236592
36	H	6.375573150911	12.904082442197
37	H	12.224349260232	11.355119696456
38	H	12.123662542450	12.981920529727
39	H	12.013937200755	11.389333884557
40	H	14.585735869503	11.963862224398
41	H	9.533155306531	12.375030472604
42	H	9.368350336611	11.817236880176
43	H	14.592611517072	12.140397756246
44	H	12.971400018192	14.602232402077
45	H	11.125073519037	9.692864118663
46	H	12.564989134358	9.503094366955
47	H	11.365502119455	14.647162317589
48	H	11.897426791773	13.009315635587
49	H	15.330143540001	11.779809384153
50	H	7.407363410080	11.496085096903
51	H	8.283863718937	13.123401548119
52	H	9.470505858687	16.031475540478
53	H	14.905155715488	15.535059594631
54	H	14.359184527495	8.390258899194
55	H	9.351121678275	8.327689033816
56	H	12.792469639752	9.664642717700
57	H	11.600373095833	15.239075267009
58	H	13.012807252093	14.391548162621
59	H	12.667883387786	9.132250111457
60			

1	H	15.240334024842	12.277126676405	9.211376785104
2	H	16.661686000381	11.972926880580	14.243003987144
3	H	7.645579309510	10.354915828923	12.589105535597
4	H	7.490686137152	11.950612599376	9.820256522223
5	H	10.700599333138	16.325802365861	13.807381205766
6	H	13.762520264432	16.596382184273	12.035504850751
7	H	13.259472478337	7.558833875581	11.916997237716
8	H	9.736216347032	8.250550464031	12.091580972988
9	H	11.396270191715	10.410147867054	16.496619658193
10	H	12.582556304847	14.369118780936	16.495633047040
11	H	11.611745235741	13.956325699828	7.679352069780
12	H	12.066303330076	10.338098641767	7.279652442233
13	H	16.536772609238	12.022773399688	10.062464529004

Coordinates of the $[\text{Al}(\text{H}_2\text{O})_{42}]^{3+}$ cluster in S_6 symmetry after annealing.

127

27	A1	11.888684583027	12.102526619069	12.043752294716
28	O	16.701945170863	10.724241867080	9.077293481958
29	O	12.841720617915	12.676487035984	16.161162101848
30	O	11.549838901656	11.652904098258	6.489653812816
31	O	15.092098785381	6.881247068376	10.122013327431
32	O	15.567115192446	10.800775177920	17.474372482806
33	O	6.375890146897	10.542801973891	13.723802669247
34	O	11.277496140022	7.307473172579	6.530563259502
35	O	17.209391411594	14.747384869104	9.285158961707
36	O	9.870750880369	5.754027487881	13.035316825566
37	O	10.087579351000	12.613676232781	16.321077975270
38	O	8.491240592597	13.765685635607	7.154508012061
39	O	15.499915431944	14.252523569250	7.238075894524
40	O	12.958677287066	10.738181542205	18.049377341304
41	O	9.168506222055	10.412273948105	7.253809964691
42	O	13.197476354866	17.468385475190	9.274209438343
43	O	8.249907017512	10.502635986184	15.762956959273
44	O	16.798795602688	9.299010910543	15.609824407800
45	O	7.558263337007	15.483695057676	11.720616103642
46	O	11.795108755882	9.280486143335	5.046750353599
47	O	7.290106069276	13.560879778482	9.691445194370
48	O	15.442487575900	13.678583708992	17.049457301630
49	O	13.698139367619	12.226507060927	8.118118694303
50	O	12.466543266263	15.861230942916	19.627467163987
51	O	10.876998129439	16.666782211124	15.052093342353
52	O	10.425359841006	11.239684823782	13.032335050077
53	O	13.201185903604	11.484205014779	13.453211681725
54	O	10.565179397911	12.874700199734	10.744648387519
55	O	12.152842104951	10.480912000731	10.938924998350
56	O	13.291639456599	12.958068714148	10.905676419190
57	O	11.694991567718	13.764110521679	13.072172415794
58	O	10.490529220078	8.498201550336	13.443705077696
59	O	15.404691526177	12.878404163609	13.477350935128

1			
2			
3			
4			
5			
6			
7	0	8.590702055573	11.081401562975
8	0	14.338740259285	9.171560123590
9	0	13.030964131260	15.589148476825
10	0	9.615832183455	14.319929920227
11	0	8.170174283359	12.526420700356
12	0	13.192153603272	8.868958825982
13	0	10.209894840604	15.602316220878
14	0	9.987661537032	8.890451153457
15	0	15.466307238443	11.689791869312
16	0	13.931370928037	15.251902488882
17	H	16.889875581404	10.756777175346
18	H	17.398619526174	10.189215521842
19	H	11.851012414671	12.795237191534
20	H	12.951417943184	12.232124970534
21	H	11.571840347706	12.345731954969
22	H	12.317096598654	11.858980350616
23	H	15.608055828543	6.384994535641
24	H	14.307316064912	6.288197064277
25	H	15.600627059972	11.790280323487
26	H	14.581574677606	10.612129259117
27	H	5.605874778396	10.162802518164
28	H	6.325538376524	10.181178655225
29	H	12.019517578190	6.676884391955
30	H	11.593683907192	8.122689577960
31	H	17.978380040412	14.116522928806
32	H	16.741926850836	14.804906786508
33	H	10.195451077577	6.684952640855
34	H	10.186213261975	5.258671127998
35	H	9.741857118871	12.829094388567
36	H	9.586371549620	11.802994015064
37	H	8.702393468764	12.841310744179
38	H	9.355836045915	14.270839837608
39	H	14.885496205311	13.508559395741
40	H	16.157504262476	14.321920649352
41	H	12.822220955528	11.478648563614
42	H	12.248778594628	10.069779241805
43	H	10.056187965870	10.803071550212
44	H	9.360534589784	9.504825372728
45	H	13.582817844143	17.117000966948
46	H	12.329218945249	17.866941186576
47	H	7.673817990747	10.465052119967
48	H	8.634552821569	9.570358886798
49	H	17.525457522476	8.907328339386
50	H	16.355649224432	9.943934604986
51	H	7.463436172273	14.701280574304
52	H	7.269595763092	16.232925251093
53	H	11.873121926159	10.138730707890
54	H	12.533198900534	9.269809009755
55	H	7.511448751684	12.644200976063
56	H	7.760697108007	13.687292319567
57	H	16.143773276669	13.557112820777
58	H	14.550755849571	13.482160377669
59	H	14.248155393074	11.422991974896
60			

1	H	13.395577434709	12.448691919988	9.037291130730
2	H	12.713027599723	14.919051584075	19.547588935512
3	H	13.232509694547	16.353564198862	19.223966370595
4	H	11.796478976636	16.452740404157	14.795112755769
5	H	10.529574975270	17.277012669527	14.316426350628
6	H	9.486288712983	11.657689085817	12.981951844469
7	H	13.256985717153	10.489213609909	13.664580776288
8	H	10.347400441474	13.852731091383	10.833368146777
9	H	11.387079595750	9.852210145995	10.785071450006
10	H	14.242570504579	12.538799808108	10.962132189433
11	H	12.460511802932	14.199533562523	13.529554326569
12	H	10.377016102707	10.257133121542	13.223110936407
13	H	14.134563322999	11.904067779533	13.482761726451
14	H	9.761159286170	12.360744639968	10.456933537400
15	H	13.002383545577	9.915980536676	11.026547934016
16	H	13.313174817786	13.972033457633	10.957847921064
17	H	10.820711329083	13.971927039851	13.619125392613
18	H	11.480595568593	8.505489683143	13.608711868489
19	H	15.007134144707	13.792493267358	13.517622253016
20	H	9.089130680419	10.307768758456	10.305490043262
21	H	14.973559163252	9.934197117839	11.279781166055
22	H	12.052011644414	15.586378071777	11.396662246510
23	H	9.718323517237	13.740647910745	15.211470348768
24	H	10.072589641805	8.304355245267	14.338494029750
25	H	16.182694331908	12.921899477236	14.108415759536
26	H	8.718128486714	10.949287517381	8.921347293878
27	H	14.662604604062	8.406508909581	10.807806705867
28	H	13.142365371153	16.257018942333	10.491010142740
29	H	9.875309466174	15.240543902299	14.678926283759
30	H	8.368989956290	13.324487581706	13.391753095340
31	H	13.733154835540	8.736659520950	12.955680138869
32	H	9.303313401590	15.575952685893	11.538966137089
33	H	9.935854117205	8.475158419802	11.606624029901
34	H	15.950603313733	12.109771092982	11.800770643342
35	H	13.821927488432	15.697857364103	12.893954479602
36	H	7.389084324273	12.072190026019	13.233699640980
37	H	13.674017469761	8.409057003141	14.531515538570
38	H	10.020615814627	16.087869656315	10.250008504735
39	H	9.760255949214	8.235232800638	9.999587083722
40	H	16.056817158531	11.517617063020	10.237951401553
41	H	14.395237485482	15.863404726727	14.402289027200
42				
43				
44				
45				
46				
47				
48				
49				
50				
51				
52				
53				
54				
55				
56				
57				
58				
59				
60				